Ecotoxicology and Environmental Safety 288 (2024) 117385

Contents lists available at ScienceDirect

Ecotoxicology and Environmental Safety

journal homepage: www.elsevier.com/locate/ecoenv

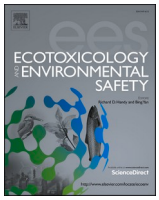

Fluoride induces immune-inflammatory disorder in the kidneys via histone lysine crotonylation in vivo

Jingwen Zheng [a,1], Qian Wang [a,1], Kangjie Xu [a], Mingyue Ma [a], Zhengdong Wang [b], Zhenxiang Sun [b], Shuang Yang [a], Xinyue Wang [a], Nan Yan [c,*], Xiaoxu Duan [a,*]

[a] Department of Toxicology, School of Public Health, Shenyang Medical College, Shenyang 110034, PR China
[b] Department of Human Anatomy, Shenyang Medical College, Shenyang 110034, PR China
[c] Department of Medical Applied Technology, Shenyang Medical College, Shenyang 110034, PR China

ARTICLE INFO

Keywords:
Fluoride
Kidney
Immune
Inflammation
Histone lysine crotonylation

ABSTRACT

Fluoride is an essential trace element for human. Adequate levels of fluoride are crucial for maintaining skeletal growth, but excessive fluoride exposure entering the body can cause renal damage, including damaged renal tubules and impaired renal function. However, the mechanism on fluoride-induced kidney injury remains unclear. This study aimed to explore the immune-inflammatory imbalance induced by fluoride and its possible mechanism in the kidneys. Mice were exposed to sodium fluoride (NaF) (0, 25, 50 and 100 mg/L) for five months. The results showed that NaF increased the renal weight and renal index. The NaF-treated groups exhibited higher serum creatinine (Cre), blood urea nitrogen (BUN), albumin (ALB) total protein (TP) levels. Further, NaF increased reactive oxygen species (ROS) levels, lipid peroxidation (LPO) levels and malondialdehyde (MDA) level. Superoxide dismutase (SOD) activity was reduced and glutathione (GSH) activities were reduced in fluoride-treated group. NaF treatment also downregulated the nuclear factor E2-related factor (Nrf2) protein and its downstream enzymes heme oxygenase-1 (HO-1) and NAD(P)H: Quinone Oxidoreductase 1 (NQO1) in the kidneys. Further, NaF shifted Th1/Th2 balance toward Th1 bias. Similarly, NaF exhibited increased macrophages and augmented M1 differentiation but suppressed M2 differentiation. The renal inflammatory response was also induced by fluoride via activation of the NOD-like receptor family pyrin domain containing 3 (NLRP3) inflammasome and increase of the pro-inflammatory factors tumour necrosis factor-α (TNF-α), transforming growth factor-β (TGF-β), interleukin-6 (IL-6) and interleukin-18 (IL-18). In addition, NaF treatment reduced the expression of the histone 2B lysine 12 crotonylation (H2BK12cr) and H4K8cr proteins as well as decreased the histone acetyltransferase P300 protein. NaF incresed the protein expression of histone decrotonylation enzyme sirtuin1 (sirt1) and histone deacetylase 3 (HDAC3) and upregulated HDAC2 protein. These findings demonstrate that fluoride exposure induces renal dysfunction and oxidative injury, affects M1/M2 polarization and Th1/Th2 differentiation, and promotes the inflammatory response via histone lysine crotonylation, ultimately resulting in nephrotoxicity.

1. Introduction

Fluoride is an essential trace element widely present in the earth's crust. The input of rocks and fluorine-containing minerals is the main source of fluoride in nature, and with the dissolution of rocks and minerals, rainfall, and the discharge of untreated or incompletely treated fluorine-containing wastes, fluoride would enter surface water or groundwater (Solanki et al., 2022). It plays a vital role in various physiological activities (Liu et al., 2023). Adequate levels of fluoride are crucial for maintaining skeletal growth and coordinating the calcium and phosphorus balance (Wang et al., 2022a, 2022b, 2022c, 2022d). However, prolonged excessive intake of fluoride can not only damage osseous tissues, bones and teeth (Piesiak-Pańczyszyn et al., 2023), but can also impact the nervous system (Chen et al., 2023), cardiovascular system (Yan et al., 2021), reproductive system (Chaithra et al., 2020) and immune system (Wang et al., 2022a, 2022b, 2022c, 2022d). Thus,

* Corresponding authors.
E-mail addresses: yannan369@163.com (N. Yan), duanxiaoxu@symc.edu.cn (X. Duan).
[1] Jingwen Zheng and Qian Wang contributed to this article equally and are co-first authors.

https://doi.org/10.1016/j.ecoenv.2024.117385
Received 14 August 2024; Received in revised form 18 November 2024; Accepted 19 November 2024
Available online 23 November 2024
0147-6513/© 2024 The Author(s). Published by Elsevier Inc. This is an open access article under the CC BY-NC license (http://creativecommons.org/licenses/by-nc/4.0/).

excessive intake of fluoride has become a global public health concern. The kidneys are the primary target organ for fluoride toxicity (Wu et al., 2021). Toxicological and epidemiological studies have also found that fluoride can cause renal toxicity, including damaged renal tubules, reduced glomerular filtration rate, and impaired renal function (Shao et al., 2020; Liu et al., 2005). Therefore, exposure to higher concentrations of fluoride could contribute to kidney damage, ultimately leading to chronic kidney disease (CKD) (Dharmaratne, 2019). The main mechanisms of fluoride nephrotoxicity include the inhibition of enzymatic activity (Kolisnyk et al., 2021), dysfunction of mitochondrial function (Aulestia et al., 2020), promotion of oxidative stress (Wang et al., 2022a, 2022b, 2022c, 2022d), acceleration of cell apoptosis (Zhang et al., 2023) and disruption of autophagy (Ma et al., 2021). Inflammation and the immune response also play a role in nephrotoxicity (Zuk and Bonventre, 2016).

Growing evidence demonstrates that the kidneys, which are not an immune organ, contain many immune cells, including dendritic cells, macrophages, natural killer cells, B cells and T cells; thus, the kidneys play a key role in balancing immunity and tolerance (Suárez-Fueyo et al., 2017). Duan et al. found that the environmental poison arsenic increased the mRNA levels of the renal Th1 cytokine interferon-gamma (IFN-γ) and the Th2 cytokine interleukin 13 (IL-13) in the kidneys and induced a tendency towards Th1, which is associated with kidney injury (Duan et al., 2022). Chow et al. also found that kidney macrophage accumulation ($CD68^+$cells) and activation ($CD68^+CD169^+$cells) occurred in equivalent diabetes mice (Chow et al., 2007). In addition, inflammation plays a pivotal role in the pathophysiological processes of kidney diseases (Kimura et al., 2017). The NOD-like receptor family pyrin domain containing 3 (NLRP3) inflammasome, which is composed of the sensing protein NLRP3, apoptosis-associated speck-like protein containing a CARD (ASC), and the downstream protein-cleaving enzyme cysteinyl aspartate specific proteinase-1 (caspase-1), plays a crucial role in regulating inflammation and immune responses (Zhang et al., 2021). Experimental studies have shown that sodium fluoride (NaF) at doses of 0.25, 1 and 2 mmol/L for 24 hours can increase the mRNA and protein expression of NLRP3, caspase-1, gasdermin D (GSDMD) and IL-1β in BV2 cells, suggesting that fluoride induces NLRP3 inflammasome activation (Zhang et al., 2024). Although the overall evidence supports the link between immuotoxicity and fluoride exposure, the underlying molecular mechansisms remain to clarified.

Protein posttranslational modification (PTM), a recently identified epigenetic phenomenon, plays an essential role in a series of physiological and pathological processes, including gene expression and regulation, cell growth, and metabolism (Yu et al., 2020; Fang et al., 2021). Lysine crotonylation (Kcr) is a newly identified modification, similar in structure to histone acetylation, that plays an important role in activating transcription and signalling pathways (Ntorla and Burgoyne, 2021).A previous study confirmed that the classic histone acetyltransferase CREB-binding protein (CBP) and its closely related p300 protein (CBP/P300) and MOF are also involved in histone lysine crotonylation (Sabari et al., 2015). The silent information regulator sirtuin 1 (Sirt1) and class I histone deacetylases (HDACs) have been found to be the primary histone decrotonylases (Fellows et al., 2018a, 2018b). Sirt1 can activate nuclear factor erythroid 2-related factor (Nrf2) to modulate IL-1β, interleukin-6 (IL-6) and tumour necrosis factor-α (TNF-α), ultimately regulating inflammation (Singh and Ubaid, 2020). Accumulating evidence indicates that HDACs are involved in the regulation of inflammation and the immune response (Mohammadi et al., 2018; Fellows et al., 2018a, 2018b). Yang et al. also found that after Toxoplasma gondii (T. gondii) infection in porcine alveolar macrophages (3D4/21 cells), the histone lysine crotonylation of 3D4/21 cells was downregulated, which was reflected by the inhibition of H2BK12cr epigenetics and nuclear factor-kappa B (NF-κB) activation. The authors also reported that a decrease in histone Kcr modification promotes macrophage proliferation (Yang et al., 2021). These results suggest that histone lysine crotonylation can regulate immune and inflammatory responses. Moreover, histone lysine crotonylation participates in a number of renal injuries and diseases. In the study by Li et al., histone Kcr of tubular epithelial cells was found to be abnormally elevated in a renal fibrosis model. Additionally, a crotonyl-CoA-producing enzyme acyl-CoA synthetase short-chain family member 2 (ACSS2) was found to remarkably increase histone 3 lysine 9 crotonylation (H3K9cr) levels (Li et al., 2024a, 2024b). He et al. constructed a diabetic kidney disease model and found that sodium crotonate (NaCr) significantly increased the PanKcr and histone 3 lysine 18 crotonylation (H3K18cr) proteins in the kidneys. NaCr also upregulated the levels of PanKcr and H3K18cr in a dose-dependent manner in HK-2 cells. The increase in Kcr was reversed by inhibiting the activity of the histone acetyltransferase P300 (He et al., 2024). However, to date, few studies have investigated whether histone lysine crotonylation is involved in fluoride-induced kidney injury.

Therefore, this study investigated the effects of fluoride treatment on the immune-inflammatory response in the kidneys. Specifically, M1/M2 polarization of macrophages, differentiation of Th1/Th2 cells, activation of the NLRP3 inflammasome, and the secretion of inflammatory factors were evaluated. Moreover, for the first time, the changes in histone lysine crotonylation and lysine crotonylation regulatory enzymes were evaluated to preliminarily investigate the underlying mechanism. The study is helpful to provide theoretical basis for the mechanism of fluoride-induced immune-inflammatory damage.

2. Methods

2.1. Reagents and chemicals

Sodium fluoride was obtained from Sigma Chemical Co. (St. Louis, MO, USA, 67414). Creatinine (Cre) (Cat.C011–2–1), blood urea nitrogen (BUN)(Cat.C013–2–1), total protein (TP)(Cat.A045–2–2), albumin (ALB)(Cat.A028–2–1), malondialdehyde (MDA)(Cat.A003–1–2), glutathione (GSH)(Cat.A006–2–1), lipid peroxidation (LPO)(Cat.A106–1–2) and superoxide dismutase (SOD)(Cat.A001–3-2) kits were provided by Nanjing KeyGEN Biotech. Co., Ltd. (Nanjing, China). A ROS kit was provided by ZCIBIO Technology Co., Ltd (Cat.ZC-38260, Shanghai, China). Real-time polymerase chain reaction (real-time PCR) kits were obtained from Takara Co. (Otsu Japan). RIPA lysis buffer (Cat.P0013B) and BCA protein assay kits (Cat.P0012) were supplied by Beyotime Biotechnology (Beyotime Shanghai, China). Primary antibodies against CD4 (Cat.A26036PM), CD11b (Cat.A24120), CD80 (Cat.A16039), CD206 (Cat.A21014), NLRP3 (Cat.A24294), caspase-1 (Cat.A0964), IL-1β (Cat.A22257), NQO1 (Cat.A23486), GADPH (Cat.A19056) and β-actin (Cat.AC038) were purchased from ABclonal (ABclonal, China). Primary antibodies against Kcr (Cat.PTM-502), H2Bk12cr (Cat.PTM-528), H4K8cr (Cat.PTM-522RM), H3(Cat.PTM-1002RM), sirt1 (Cat.PTM-5676), P300 (Cat.PTM-3023), HDAC2 (Cat.PTM-7219) and HDAC3 (Cat.PTM-6070) were purchased from PTM-Biolabs (PTM, China). Primary antibodies against Nrf2 (Cat.12721 T), HO-1 (Cat.43966 T) were purchased from Cell Signalling Technology Inc (Danvers, Massachusetts, USA). The corresponding secondary antibodies were purchased from Santa Cruz Biotechnology (Cat.sc-2357, Santa Cruz, CA, USA). All other chemicals were of analytical grade.

2.2. Animals and experimental procedures

Forty SPF male ICR mice (4 weeks old, weighing 12–14 g) were purchased from Liaoning Changsheng Biotechnology CO., Ltd (Benxi, China) (National Animals Use License Number: SYXK2021–0005). Animal use was approved by the Animal Use and Care Committee of Shenyang Medical College (protocol number: SYYXY2021031502). The mice were group-housed in stainless steel cages (10 mice per cage) in an air-conditioned room with a temperature of 22 ± 2℃ and a 12-h light/dark cycle, starting one week before experimental treatment. The mice were provided with standard mice chow diet and drinking water ad libitum throughout the study.

The dose of NaF was selected based on previously published studies (Ma et al., 2023), as well as our preliminary experiments. All mice were randomly divided into four groups (n=10/group) and were exposed to fluoride through drinking water for five months: (1) control group; (2) 25 mg/L NaF-treated group; (3) 50 mg/L NaF-treated group; (4) 100 mg/L NaF-treated group. The mice were weighed every week during the experimental period. At the end of the experiment, all mice were weighed and deeply anesthetized with an intraperitoneal injection of 3.3 % chloral hydrate (dissolved in normal saline). Blood was collected in vials and centrifuged (3000 x g, 4℃) for 10 min. The obtained serum was frozen at −80°C for analysis. The kidneys were promptly removed, weighed, isolated and stored at −80°C for biochemical analysis.

2.3. Calculation of the kidney index

The kidney index was calculated according to the following formula: (kidney weight/body weight)×100.

2.4. Determination of the Cre, BUN, TP and ALB levels in serum

The serum Cre, BUN, TP and ALB levels were measured using commercially available kits, according to the manufacturer's instructions. The level of Cre was finally expressed as μmol/L, the level of BUN was finally expressed as mmol/L, the level of TP was finally expressed as g/L and the level of ALB was finally expressed as g/L.

2.5. Determination of the ROS levels in the kidneys

ROS level were measured by enzyme-linked immunosorbent assay (ELISA), using commercially available high-sensitivity kits (zcibio, Shanghai) according to the manufacturers' instructions. In brief, the kidney of mice was washed with PBS to removed blood and clots, and then homogenized on ice with 9 ml saline per gram of tissue weight. Homogenate were then certrifuged at 5000 g for 10 min at 4℃ and the supernatants were used for analysis of ROS, 50 μl of Standardized product and 50 μl test samples were added in ELISA plate respectively. 100 μl of streptavidin-HRP solution was added to each well and incubated for 60 min at 37℃, followed by five gentle washing with wash buffer. 50 μl of substrate A and B was added, mixed by shaking and incubated 15 min in dark environment. Reaction was terminated by adding 50 μl of stop solution. Finally, optical density was measured at 450 nm by an automatic microplate reader (SpectraMax M5). The level of ROS was finally expressed as U/ml.

2.6. Determination of MDA, LPO, SOD and GSH levels in the kidneys

The kidney of mice was washed with normal saline to removed blood and clots, and then homogenized on ice with 9 ml saline per gram of tissue weight. Homogenate were then certrifuged at 3500 g for 10 min at 4℃ and the supernatants were used for analysis of MDA, LPO, SOD and GSH in the kidney. The MDA, LPO, SOD and GSH levels in the kidneys were measured using commercially available kits, according to the manufacturer's instructions. The level of MDA was finally expressed as nmol/mgprot, the level of LPO was finally expressed as μmol/g prot, the level of SOD was finally expressed as U/mg prot and the level of GSH was finally expressed as μmol/L.

2.7. Histopathology and Immunohistochemical staining of the kidneys

The mice was treated by transcardial perfusion with PBS and 4 % paraformaldehyde, kidney was harvested and embedded in paraffin. 5 μm-thick sections were deparaffinized in xylene and rehydrated in graded alcohol and stained with hematoxylin and eosin for histopathologic analysis.

Immunohistochemical analysis was performed to detect the expression of CD4, CD11b, CD80 and CD206 in the kidneys. Endogenous peroxidase activity was blocked by absolute methanol containing 3 % hydrogen peroxide. Then, the sections were incubated overnight at 4°C with the primary antibodies anti-CD4 (1:200), anti-CD11b (1:200), anti-CD80 (1:100) and anti-CD206 (1:200). Subsequently, the sections were incubated with the secondary antibodies for 30 min at room temperature. Then, the sections were stained with 3,3-diaminobenzidine (DAB) and counterstained with haematoxylin. After dehydration and drying, the sections were mounted with neutral gum and observed under a microscope (Biodirect Inc., Nikon, Japan), and the sites of brownish yellow particle precipitation were judged as positive.

2.8. Total RNA isolation and real-time PCR analysis

Total RNA of kidney was isolated from the kidneys with TRIzol reagent (Invitrogen, USA), and first-strand cDNA was synthesized from a 1 μg-aliquot of the total RNA using the oligo-dT primer and reverse transcriptase. Primers for genes were designed by PRIMER 3 software and synthesized by Sangon Biological Engineering technology (Shanghai, China) as shown in Table 1. Then, PCR amplification was performed using a SYBR Premix Ex*Taq*II kit (Takara, Japan). PCR was performed using the following thermal cycling conditions: 95°C for 30 s, followed by 40 cycles of denaturing at 95℃ for 5 s and annealing at 60℃ for 30 s. $2^{-\Delta\Delta Ct}$ values were calculated to represent the expression levels of the different target genes, the final values presented were expressed as folds of control.

2.9. Western blot analysis

Total protein was extracted from the kidneys by a commercial kit and the protein concentration was quantified by a bicinchoninic acid (BCA) protein kit (Beyotime, Shanghai, China) using bovine serum albumin as the protein standard. A nuclear-cytosol extraction kit (Beyotime Biotechnology, Shanghai) was used to isolate the nuclear and cytosol fractions. We examined the expression levels of Nrf2 (1:1000) in the cytoplasm and nucleus, as well as NLRP3 (1:1000), caspase-1 (1:1000), IL-1β (1:1000), HO-1 (1:1500), NQO1 (1:1000), Kcr (1:500), H2BK12cr (1:1000), H4K8cr (1:1000), sirt1 (1:1000), p300 (1:500), HDAC2

Table 1
Primer sequences for real-time qPCR.

Gene	Primers sequences (5'-3')	Product (bP)
Tbet (NM 019507.2)	F: 5′- CAACCAGCACCAGACAGAGA−3′ R: 5′-TCCACCAAGACCACATCCAC−3′	129
Ifn-γ (NM 008337.4)	F: 5′-AAGCGTCATTGAATCACACCTG−3′ R: 5′-TGACCTCAAACTTGGCAATACTC−3′	92
Gata3 (NM 001417048.1)	F: 5′-CTCGGCCATTCGTACATGGAA−3′ R: 5′-GGATACCTCTGCACCGTAGC−3′	134
Il−4 (NM 021283.2)	F: 5′-AAAATCACTTGAGAGAGATCATCGG−3′ R: 5′-GTTGCTGTGAGGACGTTTGG −3′	97
Tnf-α (NM 013693.3)	F: 5′-CCTGTAGCCCACGTCGTAG−3′ R: 5′-GGGAGTAGACAAGGTACAACCC−3′	148
Tgf-β (XM 036152883.1)	F: 5′-TGTGGAACTCTACCAGAAATATAGC−3′ R: 5′-GAAAGCCCTGTATTCCGTCTC−3′	152
Il−6 (NM 001314054.1)	F: 5′-CTGCAAGAGACTTCCATCCAG−3′ R: 5′-AGTGGTATAGACAGGTCTGTTG−3′	131
Il−18 (XM 036154619.1)	F: 5′-AGACCTGGAATCAGACAACTTT−3′ R: 5′-TCAGTCATATCCTCGAACACA−3′	117
Nlrp3 (XM 036156549.1)	F: 5′-GCCTTGAAGAAGAGTGGATGG−3′ R: 5′-CTGCGTGTAGCGACTGTTG−3′	176
Caspase−1 (NM 009807.2)	F: 5′-GGACCCTCAAGTTTTGCCCT−3′ R: 5′-AACTTGAGCTCCAACCCTCG−3′	161
Il−1β (XM 006498795.5)	F: 5′-TGACCTGGGCTGTCCTGATG−3′ R: 5′-GGTGCTCATGTCCTCATCCTG−3′	160
Gapdh (NM 001411843.1)	F:5′-TGTGTCCGTCGTGGATCTGA−3′ R: 5′-TTGCTGTTGAAGTCGCAGGAG−3′	150

(1:1000), HDAC3 (1:1000) in the cytoplasm. Forty-five micrograms of total protein was boiled with the sample loading buffer for 3 min at 100℃ before being separated by 7.5–10 % SDS-PAGE. After electrophoresis, proteins were transferred to a 0.22 μM polyvinylidene fluoride (PVDF) membrane (Amersham, Buckinghamshire, UK). The blots were placed in blocking solutions (PBS containing 80 mmol/L Na_2HPO_4, 25 mmol/L $NaH_2PO_4{\cdot}2\ H_2O$ and 100 mmol/L NaCl, 0.1 % Tween 20, and 5 % skim milk) for 2 h at room temperature. the membranes were probed with primary antibodies against NLRP3, caspase-1, IL-1β, Nrf2, HO-1, NQO1, Kcr, H2BK12cr, H4K8cr, sirt1, p300, HDAC2, HDAC3, H3 and β-actin at 4℃ overnight, respectively. On the other day, the membranes were washed with TBST five times for seven minutes each time, and then incubated with the corresponding secondary antibodies (1:5000) for 2 h at room temperature. Subsequently, the membranes were washed with TBST five times for seven minutes each time. Finally, Blots were detected with chemiluminescence reagents (PicoWest Super Signal, Pierce Biotechnology, USA) and visualized using an electrophoresis gel imaging analysis system (MF-ChemiBIS 3.2, DNR Bio-Imaging Systems, Israel). Grayscale quantitative analysis of the protein bands was performed by Image J software. H3, β-actin and GAPDH were used as the internal controls.

2.10. Statistical analysis

The data are expressed as the mean ± SD. All analyses were performed using SPSS 25.0 statistical analysis software. Comparisons among groups were performed using one-way analysis of variance (ANOVA) with LSD post-hoc tests. $P<0.05$ was considered to be statistically significant.

3. Results

3.1. General characteristics of the study mice

All experimental mice showed normal activity and survived until the end of the experiment. As shown in Fig. 1, the kidney weight and kidney index in the 25 mg/L NaF-treated group were significantly increased ($P<0.05$).

3.2. Effects of fluoride exposure on histomorphological alterations and kidney function in mice

We performed H&E stain to investigate the histopathologic changes in the kidney. The representative histopathological results of H&E staining of kidneys are presented in Fig. 2. In the control group, renal tubular epithelial cells were well-arranged, glomeruli were intact and the basement membrane was evenly distributed. Compared with the control group, fluoride-treated mice showed kidney tubular epithelial cells swollen, nucleus and cell debris shedding and infammatory cells infltrating. With the increase of dose and time, we also observed subsequently extensive disruption of the kidney architecture.

In addition, the serum Cre, BUN, TP and ALB levels were evaluated to examine the degree of functional kidney damage. As shown in Fig. 2B, compared with the control group, the level of CRE was increased in response to fluoride exposure in a dose-dependent manner ($P<0.05$). The BUN and ALB levels were significantly higher in all NaF-treated groups as compared to the control group ($P<0.05$). Moreover, the 50 and 100 mg/L NaF treatments upregulated the TP level in the kidneys, as compared to the control group ($P<0.05$).

3.3. Effects of fluoride exposure on oxidative injury in the kidneys

Oxidative stress could contribute greatly to fluoride-induced toxicity, so we detected the oxidative injury in kidney. As shown in Fig. 3, compared to the control group, the 25 and 100 mg/L fluoride treatments significantly increased the levels of ROS ($P<0.05$). The level of MDA in the kidneys was also markedly increased in the 100 mg/L NaF-treated group when compared with the control group and the 25 and 50 mg/L NaF-treated groups ($P<0.05$). In contrast, the LPO levels were increased significantly by 57.64 %, 57.85 % and 49.52 %. Moreover, there was a notable decrease in SOD activity in the 100 mg/L NaF-treated group ($P<0.05$). In addition, there was a clear decrease in the GSH activity in the kidneys after fluoride exposure, as compared to the control group ($P<0.05$).

In addition, the Nrf2 pathway was detected by western blot because Nrf2 pathway is a classic antioxidant response element closely related to oxidative stress. As shown in Fig. 4, compared to the control group, NaF treatment significantly increased Nrf2 levels in the nucleus, with a corresponding decrease in the cytoplasm ($P<0.05$). There was also

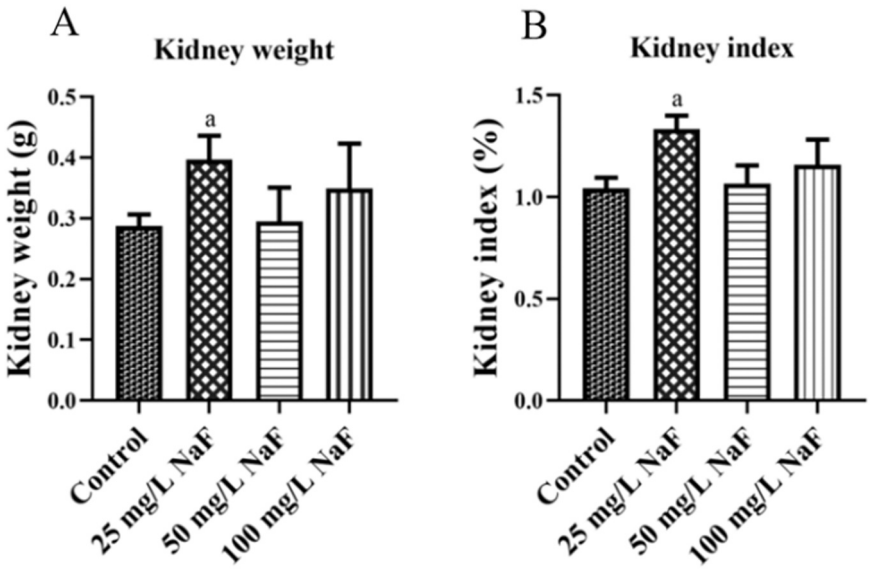

Fig. 1. Effects of fluoride exposure on kidney weight and kidney index in mice. Mice were treated with 0, 25, 50 and 100 mg/L NaF-treated by drinking water for 5 months, the kidney was promptly removed and weighted, and the kidney index was calculated. The results were expressed as the mean ± SD (n = 10). [a] $P<0.05$ compared with the control mice.

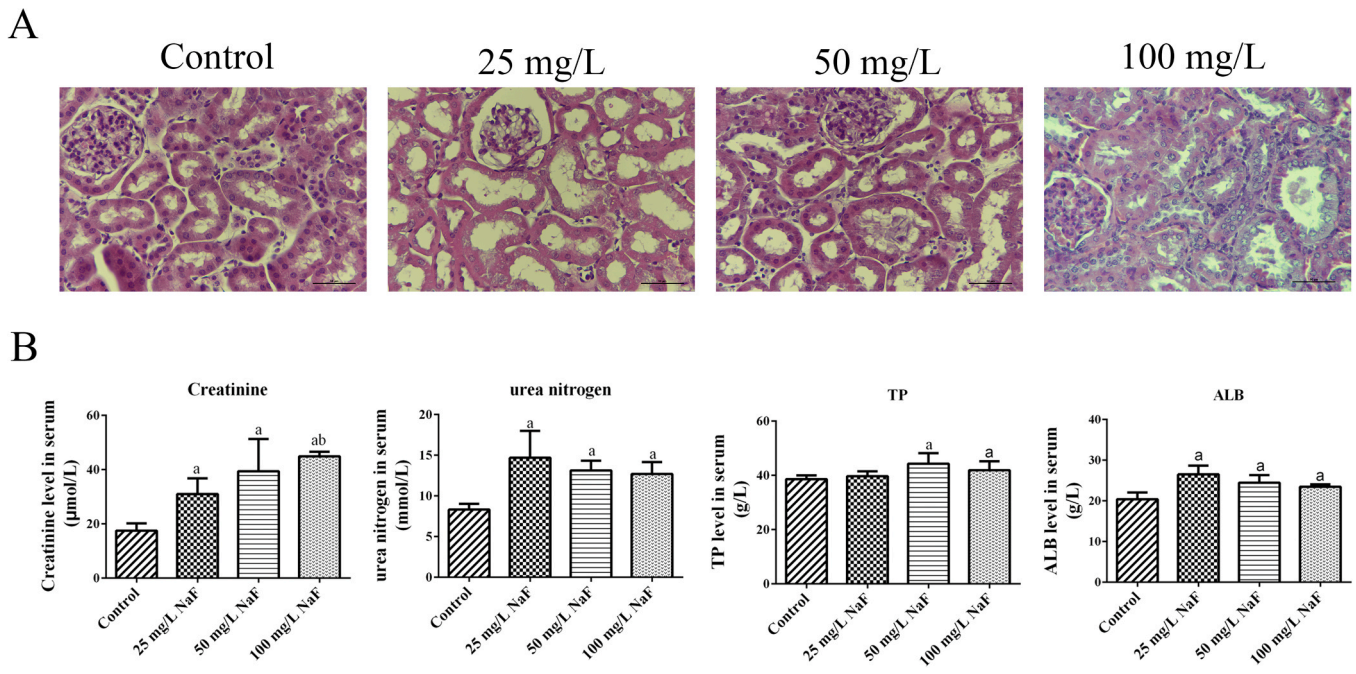

Fig. 2. Effects of fluoride exposure on histomorphological alterations and kidney function in mice. Mice were treated with 0, 25, 50 and 100 mg/L NaF-treated by drinking water for 5 months. After the treatment, (A) the histopathological changes were detected by hematoxylin-eosin (H&E) assay (original magnification: ×400). (B) Cre, BUN, TP, ALB levels in serum were measured using commercially available kits. The results were expressed as the mean ± SD (n = 6). [a] $P<0.05$ compared with the control mice. [b] $P<0.05$ compared with the 25 mg/L NaF-treated mice.

notable downregulation of its downstream enzymes HO-1 in all NaF-treated groups ($P<0.05$). Compared to the control group, the expression of NQO1 was decreased in the kidneys in the 25 and 100 mg/L NaF-treated mice ($P<0.05$). These results indicated that fluoride exposure induced oxidative injury in the kidneys.

3.4. Effects of fluoride on T-cell differentiation in the kidneys

$CD4^+$T cells play an important role in regulating the immunity. First, the number of $CD4^+$ T cells was measured by immunohistochemical staining. The results demonstrated that fluoride increased the number of $CD4^+$T lymphocytes in the kidneys (Fig. 5A). Next, the expression of specific transcription factors and cytokines of Th1 and Th2 were investigated by real-time PCR. As shown in Fig. 5, 100 mg/L NaF increased the mRNA expression of the Th1 transcription factor T-bet and cytokine IFN-γ (Figs. 5B and 5C, $P<0.05$). Compared to the control group, the levels of the Th2 transcription factor Gata3 and cytokine IL-4 were decreased in the 25, 50 and 100 mg/L NaF-treated groups (Figs. 5D and 5E, $P<0.05$). These results indicate that fluoride affected the number of $CD4^+$ T cells and induced a prominent Th1 cell advantage in the kidneys.

3.5. Effects of fluoride on macrophage polarization in the kidneys

As shown in Fig. 6, the immunohistochemical results showed that fluoride increased the expression of CD11b-stained macrophages in the kidneys. Next, the expression levels of CD80 and CD206 were measured as markers of M1 and M2 polarized macrophages. In addition, 50 and 100 mg/L NaF significantly increased the number of $CD80^+$M1-like macrophages, while the numbers of renal $CD206^+$M2-like macrophages were markedly lower in the 50 and 100 mg/L NaF-treated groups as compared to the control group.

3.6. Effects of fluoride on inflammatory response in the kidneys

Inflammatory response has been found to be one of the most important factors that contribute to fluoride-induced toxicity. Firstly, the effect of fluoride on NLRP3 inflammasome activation was explored by real-time PCR and western blot. As shown in Fig. 7, the mRNA expression levels of NLRP3, caspase-1 and IL-1β were markedly elevated in the 100 mg/L NaF-treated group ($P<0.05$). In contrast, there was notable up-regulation of the NLRP3 and caspase-1 protein levels in the kidneys of the 50 and 100 mg/L NaF-treated groups and the IL-1β protein level in the 25, 50 and 100 mg/L NaF-treated groups ($P<0.05$).

Moreover, the mRNA levels of the inflammatory cytokines TNF-α, TGF-β, IL-6 and IL-18 in the kidneys were determined by real-time PCR. As shown in Fig. 8, the mRNA levels of nephritic TNF-α, TGF-β and IL-6 were markedly elevated in the 100 mg/L NaF-treated group as compared to the control group and the 25 and 50 mg/L NaF-treated groups (Fig. 8A-C, $P<0.05$). The mRNA level of IL-18 was significantly increased in a dose-dependent manner in response to fluoride exposure (Fig. 8D, $P<0.05$). These results indicate that fluoride induced an inflammatory response in the kidneys.

3.7. Effects of fluoride on histone lysine crotonylation modification in the kidneys

As the histone lysine crotonylation modification was found to play an important regulatory part in immune imbalance and inflammation, so we observed the expression of lysine crotonylation as well as its regulatory enzyme. There was a significant up-regulation in the expression of lysine crotonylation in the kidneys of the normal relative to the fluoride-treated mice (Fig. 9A). Furthermore, the 25 and 100 mg/L NaF-treated groups exhibited significantly downregulated H2BK12cr protein expression in the kidneys as compared to the control group, and the expression of the H4K8cr protein was markedly decreased in 50 and 100 mg/L fluoride-treated groups (Fig. 9B, $P<0.05$). Next, the expression levels of lysine crotonylation-related enzymes were detected in the kidneys. As shown in Fig. 9C, the expression of the histone acetyltransferase P300 in the kidneys was decreased in the 100 mg/L NaF-treated group ($P<0.05$). Additionally, the 50 and 100 mg/L NaF treatment upregulated the levels of the renal histone decrotonylation enzyme

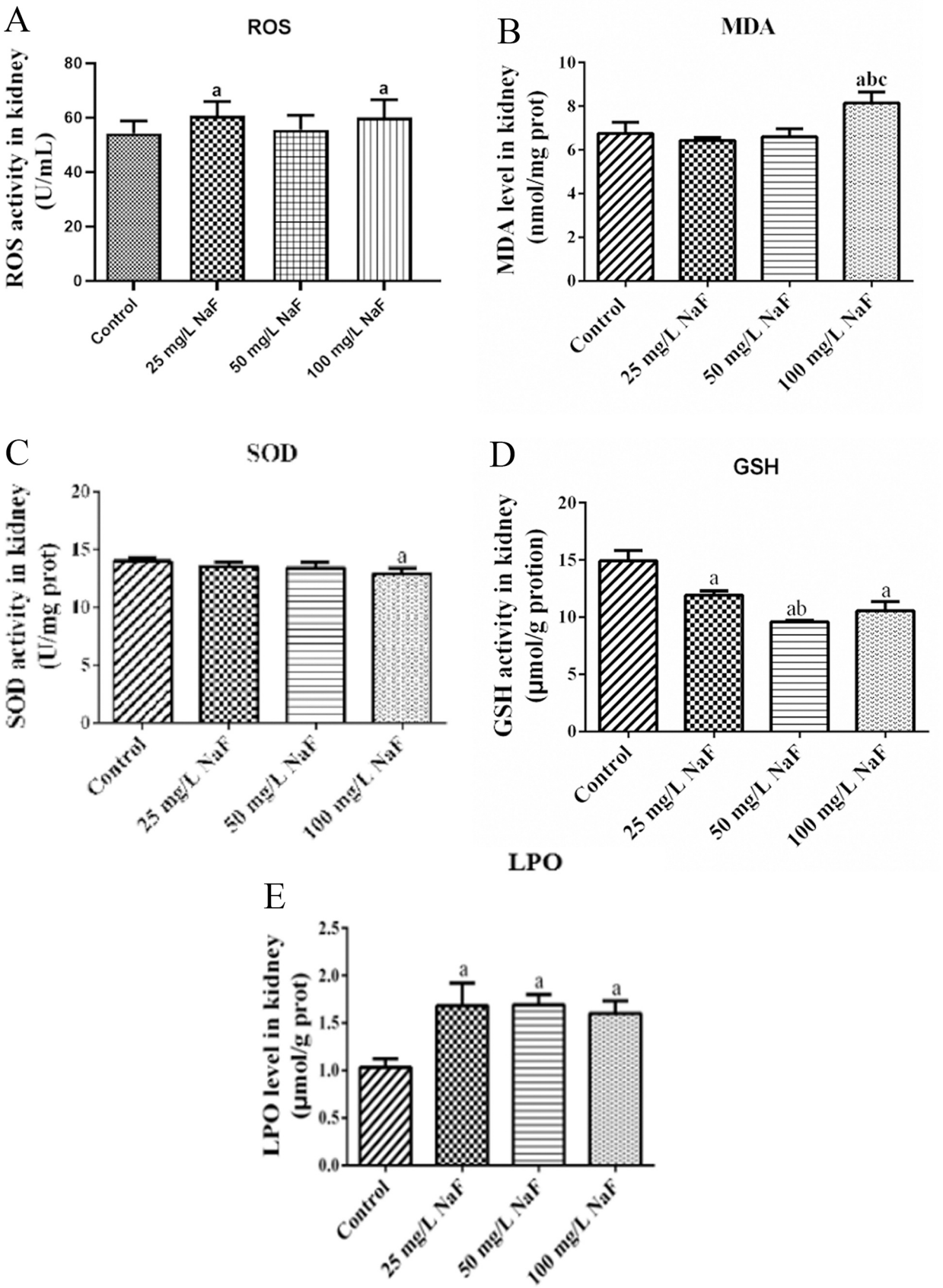

Fig. 3. Effect of fluoride exposure on oxidative stress in kidney. Mice were treated with 0, 25, 50 and 100 mg/L NaF-treated by drinking water for 5 months. After the treatment, (A) reactive oxygen species (ROS), (B)malondialdehyde (MDA), (C) superoxide dismutase (SOD), (D)glutathione (GSH) and (E) lipid peroxidation (LPO) levels in kidney were measured using commercially available kits. The results were expressed as the mean ± SD (n = 6). [a] $P<0.05$ compared with the control mice. [b] $P<0.05$ compared with the 25 mg/L NaF-treated mice. [c] $P<0.05$ compared with the 50 mg/L NaF-treated mice.

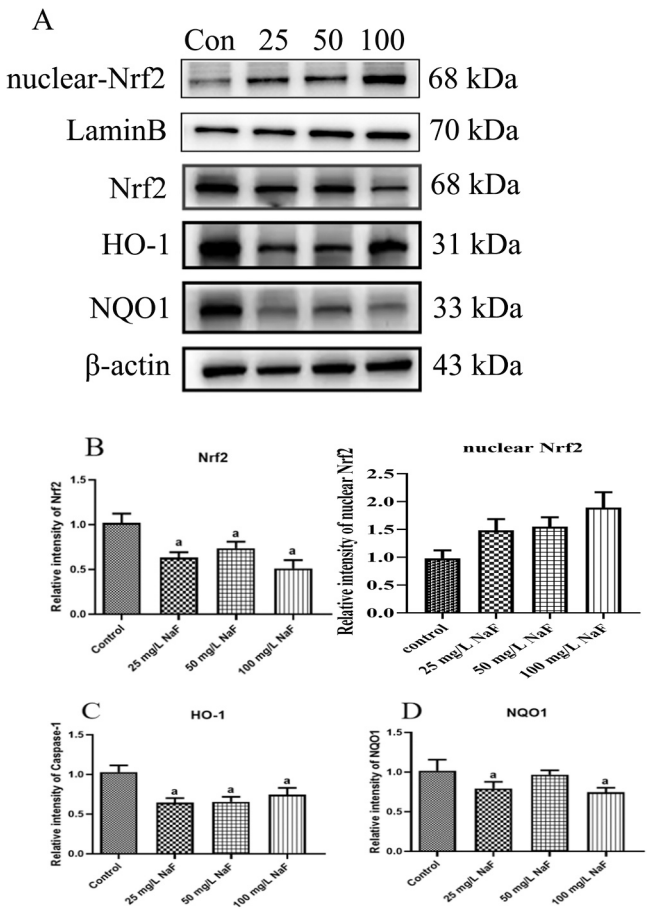

Fig. 4. Effects of fluoride on Nrf2/HO-1/NQO1 pathway in kidney. Mice were treated with 0, 25, 50 and 100 mg/L NaF-treated by drinking water for 5 months. Expression of nuclear factor E2-related factor (Nrf2), heme oxygenase-1(HO-1), NAD(P)H:Quinone Oxidoreductase 1(NQO1) in kidney were assessed by western blotting. β-actin was blotted as the loading control. The results were expressed as the mean ± SD (n = 4). [a] $P<0.05$ compared with the control mice.

Sirt1 and HDAC3 ($P<0.05$). The 25, 50 and 100 mg/L NaF-treated groups exhibited significantly up-regulated HDAC2 protein expression in the kidneys as compared to the control group. These results indicate that fluoride exposure can regulate histone lysine crotonylation modification in the kidneys.

4. Discussion

The kidneys serve as the primary route for eliminating fluoride from the body. Toxicological and epidemiological reports have demonstrated that fluoride can harm kidney function. Immunologists have discovered that the kidneys, traditionally considered a non-immune organ, also contain immune cells, including lymphocytes and macrophages, which participate in the immune response. Additionally, an immuno-inflammatory imbalance plays a role in the occurrence and development of kidney injury and diseases. Therefore, in this study, we investigated the effect of fluoride exposure on the renal immune-inflammatory response and the possible underlying mechanism.

Intake of excess fluoride can impair renal structure and function. Ten weeks of 100 mg/L NaF with drinking water induced the pathologic changes including disordered arrangement of renal tubule cells accompanied by multiple tubular cell ruptures, nucleus and cell debris shedding, slightly dilated (Hu et al., 2023). In addition, our results were corroborated by the similar findings of the kidney. Kidney damage or nephrotoxicity leads to the impairment of detoxification and excretion functions, which can be confirmed by renal markers such as Cre, BUN, TP and ALB. (Malin et al., 2019). Cre is a muscle metabolite, while BUN is the main end-product of protein metabolism. Both are excreted via glomerular filtration and are commonly used to gauge kidney function (Myers et al., 2006; Wang et al., 2020). In a study by Li et al., rats treated with 100 mg/L NaF showed significant increases in serum BUN and Cre levels, reflecting renal biochemical changes and insufficiency due to NaF exposure (Li et al., 2021a, 2021b). Similarly, Qujeq et al. discovered that oral administration of NaF at doses of 10, 20 and 30 mg/kg daily for 90 days resulted in a notable decrease in the average serum TP level and increased transaminase activity in adult rats, as compared to the control group (Qujeq et al., 2002). ALB, an early biomarker of kidney injury serves as a valuable tool for assessing early kidney toxicity from fluoride exposure. Zhao et al. observed that Wistar rats exposed to 50 mg/L NaF

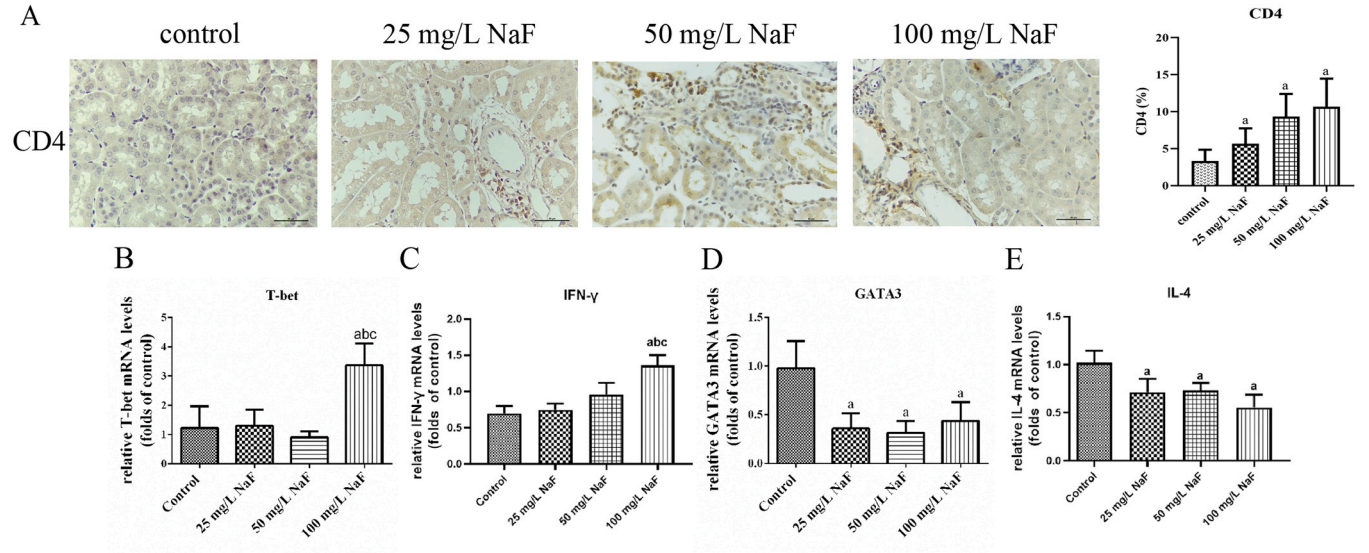

Fig. 5. Effects of fluoride on $CD4^{+}$T cell and Th1/Th2 subpopulation in kidney. Mice were treated with 0, 25, 50 and 100 mg/L NaF-treated by drinking water for 5 months. (A) Expression of CD4 in kidney by immunohistochemistry(×400 magnification), n=3, Scale bar=50 μm. Semiquantitative analysis of IHC of CD4 in kidney. The mRNA levels of (B)T-box transcription factor (T-bet), (C) interferon gamma (IFN-γ), (D) gata-binding protein 3 (GATA3) and (E) interleukin-4 (IL-4) in kidney were determined by real-time PCR. The results were expressed as the mean ± SD (n = 6). [a] $P<0.05$ compared with the control mice. [b] $P<0.05$ compared with the 25 mg/L NaF-treated mice. [c] $P<0.05$ compared with the 50 mg/L NaF-treated mice.

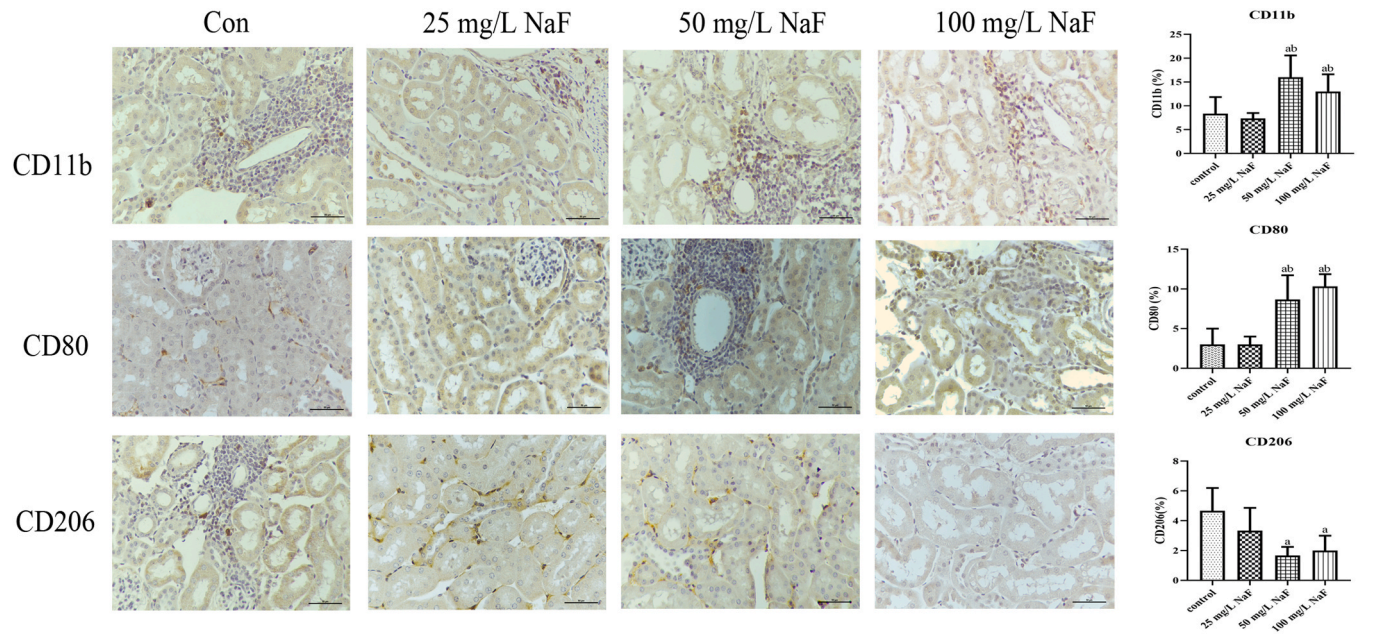

Fig. 6. Effects of fluoride on the macrophages polarization in kidney. Mice were treated with 0, 25, 50 and 100 mg/L NaF-treated by drinking water for 5 months. Expression of CD11b, CD80 and CD206 in kidney were determined by immunohistochemistry (×400 magnifcation). Scale bar=50 μm, n=3. Semiquantitative analysis of IHC of CD11b, CD80 and CD206 in kidney.

for six months exhibited reduced TP and ALB levels compared to the control group (Zhao et al., 2014). The current results demonstrated that fluoride exposure increased the serum levels of TP and ALB. The inconsistency in the current findings relative to previous reports may be related to the type of fluoridation, dose and duration. The exact cause requires further research.

One of the main mechanisms underlying fluoride toxicity is oxidative stress (Wang et al., 2022a, 2022b, 2022c, 2022d). Oxidative injury is defined as an imbalance between ROS production and antioxidant capacity. Excessive production of ROS is thought to activate the NF-κB pathway and result in the upregulation of pro-inflammatory mediators (Farooq et al., 2019), where ROS generate genotoxic end-products such as MDA and suppress antioxidant enzymes such as SOD and GSH (Chen et al., 2019; Dahdouh et al., 2023). MDA, a byproduct of lipid peroxidation, serves as a marker of oxidative stress and cellular damage (Karadogan et al., 2022). SOD is an important antioxidant enzyme that scavenges superoxide radicals, while GSH serves as a key cellular antioxidant and cofactor for detoxification enzymes (Ma et al., 2020). LPO reflects the extent of lipid peroxidation, which can lead to cellular dysfunction and organ failure (Ramasubramanian et al., 2021). Chen et al. (2015) found that carp juveniles exposed to NaF exhibited dose- and time-dependent decreases in SOD and GSH levels in the kidneys while the MDA level showed a dose- and time-dependent increase. Similarly, Nabavi et al. (2012) observed that male Wistar rats exposed to 600 ppm NaF experienced a significant decrease in the GSH level and catalase activity in the kidneys, along with suppressed SOD activity. Additionally, a notable elevation in LPO in the kidney tissues was observed upon NaF intoxication in rats. Consistent with these findings, the current results revealed obvious alterations in oxidative stress due to NaF treatment, including increased MDA contents and LPO levels and decreased SOD activities, GSH levels. In addition, ROS have also been involved in T cell subset differentiation by regulating IFN-γ and IL-17 cytokines (Aksoylar et al., 2020). Nrf2 is a central regulator of cellular resistance to oxidative stress, which could be released and translocated to the nucleus under oxidative stress, then regulates a series of antioxidant enzymes, such as HO-1 and NQO1, and plays a pivotal role in the regulation of oxidative stress, apoptosis and cancer, among others (Che et al., 2023; Weiss-Sadan et al., 2023). Consistent with the current results, Hu et al. (2021) found that 100 mg/L NaF changed the gene and protein expression levels of Nrf2, HO-1 and NQO1. These findings suggest that fluoride can induce oxidative injury.

The kidneys contain dendritic cells, macrophages, T cells and B cells. These cells participate in the immune response and play a critical role in the pathogenesis of kidney disease (Qu and Jiao, 2023). $CD4^+$T cells are crucial for immune functions. They maintain host health and prevent the occurrence and development of diseases (Sun et al., 2023). $CD4^+$T cells can also differentiate into Th1 or Th2 cell subsets. T-bet is known to promote the differentiation of Th1 cells and the production of pro-inflammatory cytokines such as IFN-γ, which can exacerbate inflammation and tissue injury (Shang et al., 2024). GATA3 is crucial for the differentiation of Th2 cells and the secretion of anti-inflammatory cytokines such as IL-4 and IL-10, which play key roles in tissue repair and the resolution of inflammation (Li et al., 2021a, 2021b). NaF induced a significant decrease in the percentages of $CD3^+$, $CD3^+CD4^+$, $CD3^+CD8^+$ T lymphocytes and $CD4^+/CD8^+$ ratio in the peripheral blood and spleen (Guo et al., 2017; Li et al., 2021a, 2021b). Peres et al. (2023) also found that $CD4^+$ T cells were activated in subclinical acute kidney injury followed by Th1 and Th2 phenotype differentiation, characterized by an increase in the production of IFN-γ and no change in the IL-4-producing Th2 phenotype in the renal cortex. Another study by Zhang et al. (2023) investigated the absolute T lymphocyte count and Th1/Treg cell imbalance in the peripheral blood of patients with end-stage renal disease. In the current study, the mRNA levels of the Th1 transcription factor T-bet and cytokine IFN-γ were dramatically increased while the Th2 transcription factor GATA3 and cytokine IL-4 levels were significantly downregulated in the kidneys after fluoride exposure. Taken together, it appears that fluoride increases the percentages of $CD4^+$T cell and induces abnormalities in Th1/Th2 cells, including polarization to Th1 subpopulations. These findings provide a deeper understanding of the fluoride-induced renal immune imbalance.

Macrophages are one of the most effective immune defence cells due to their strong ability to phagocytize and kill pathogens. They are polarized into two distinct functional phenotypes: proinflammatory (M1) and anti-inflammatory (M2) (Funes et al., 2018). CD11b is indicative of the macrophage differentiation status. CD80, expressed by macrophages and other antigen-presenting cells, serves as a marker of

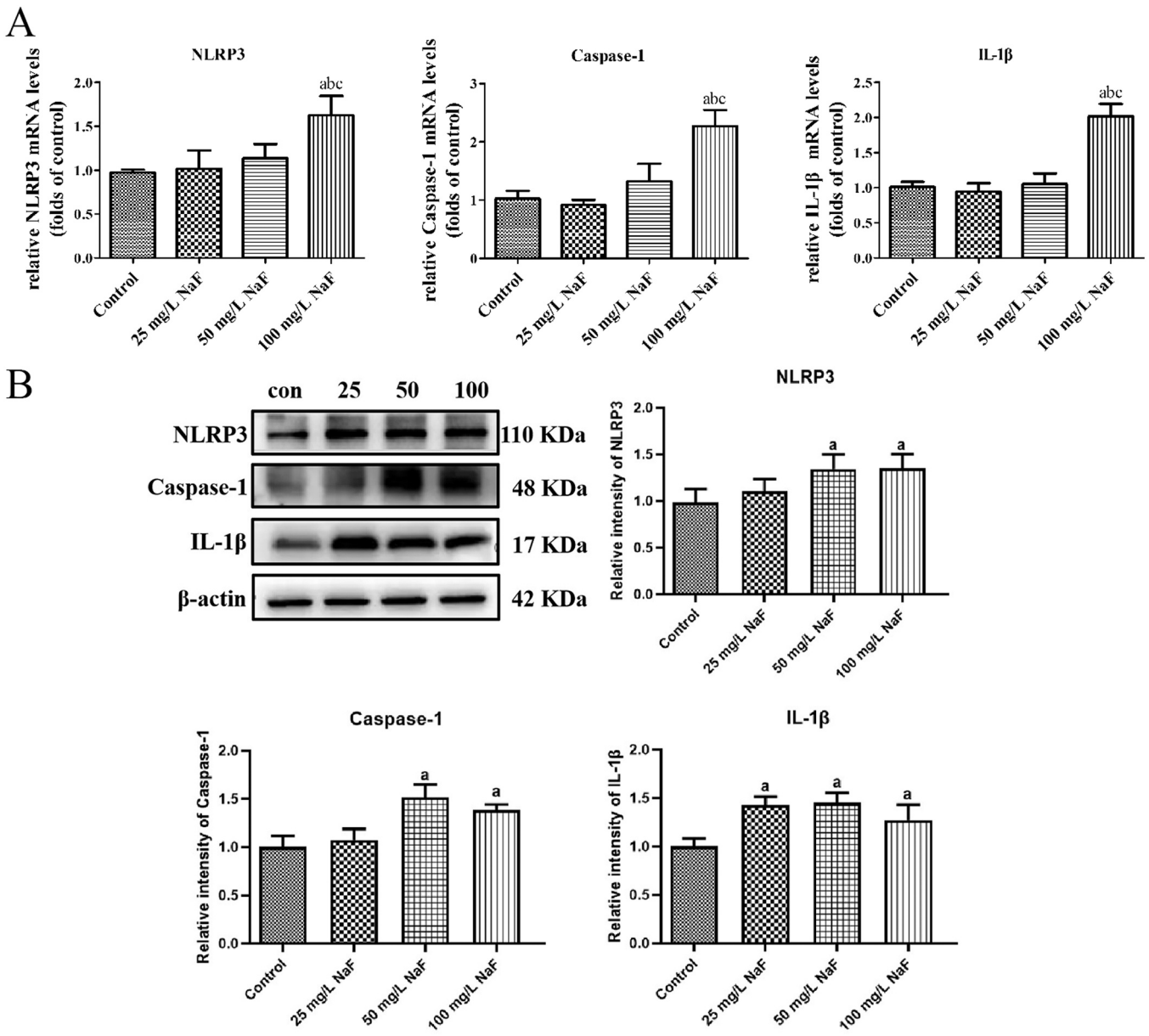

Fig. 7. Effect of fluoride on NLRP3 inflammasome in kidney. Mice were treated with 0, 25, 50 and 100 mg/L NaF-treated by drinking water for 5 months. The mRNA levels of NOD-like receptor family pyrin domain containing 3 (NLRP3),cysteinyl aspartate specific proteinase1 (caspase1) and interleukin 1β (IL-1β) in kidney were determined by real-time PCR(A). Protein expression of NLRP3, caspase-1 and IL-1β (B) in kidney were assessed by western blotting. β-actin was blotted as the loading control. Results were expressed as the mean ± SD (n = 6). [a] $P<0.05$ compared with the control mice. [b] $P<0.05$ compared with the 25 mg/L NaF-treated mice. [c] $P < 0.05$ compared with the 50 mg/L NaF-treated mice.

M1 polarization, whereas CD206 is the predominant marker for M2 macrophages, which are involved in tissue repair and anti-inflammatory processes (Shapouri-Moghaddam et al., 2018). Ma et al. (2016) found that 50 μM NaF significantly enhanced CD80 expression in splenic B cells by flow cytometric analysis. Du et al. (2022) found that 5 and 10 mM NaF exposure for four weeks resulted in an increase in the M1 macrophage marker CD86 and downregulation of the number of CD206-positive cells by immunohistochemical staining. Similarly, in the current study, there were obvious increases in CD11b and CD80 expression, as well as a decrease in CD206 in the kidneys. These results suggest that fluoride suppresses M2 differentiation but augments M1 differentiation of macrophages in the kidneys.

Chronic inflammation plays a crucial role in many renal diseases, including glomerulonephritis (Levey and Coresh, 2012), tubulointerstitial nephritis (Joyce et al., 2017) and diabetic nephropathy (Foresto-Neto et al., 2024). The NLRP3 inflammasome is a multiprotein complex (NLRP3, caspase-1 and ASC) that promotes the maturation and secretion of pro-inflammatory cytokines such as IL-1β (Fu and Wu, 2023). It triggers inflammasome assembly and caspase-1 activation in response to cellular stress and damage, playing an important role in initiating and perpetuating inflammatory responses (Xu and Núñez, 2023). Li et al., (2024a), (2024b) found that exposure to 100 mg/L fluoride significantly increased the mRNA and protein expression of NLRP3, caspase-1 and IL-1β in the testes of mice. In a diabetic nephropathy model induced by streptozocin (STZ) in rats, Wang et al. (2012) found that the accumulation of uric acid and lipids led to the activation of the NLRP3 inflammasome followed by the maturation and secretion of IL-1β and IL-18, which triggered further pro-inflammatory events, thus participating in the renal damage caused by STZ-induced diabetes in rats (Santoyo-Sanchez et al., 2013). In the current study,

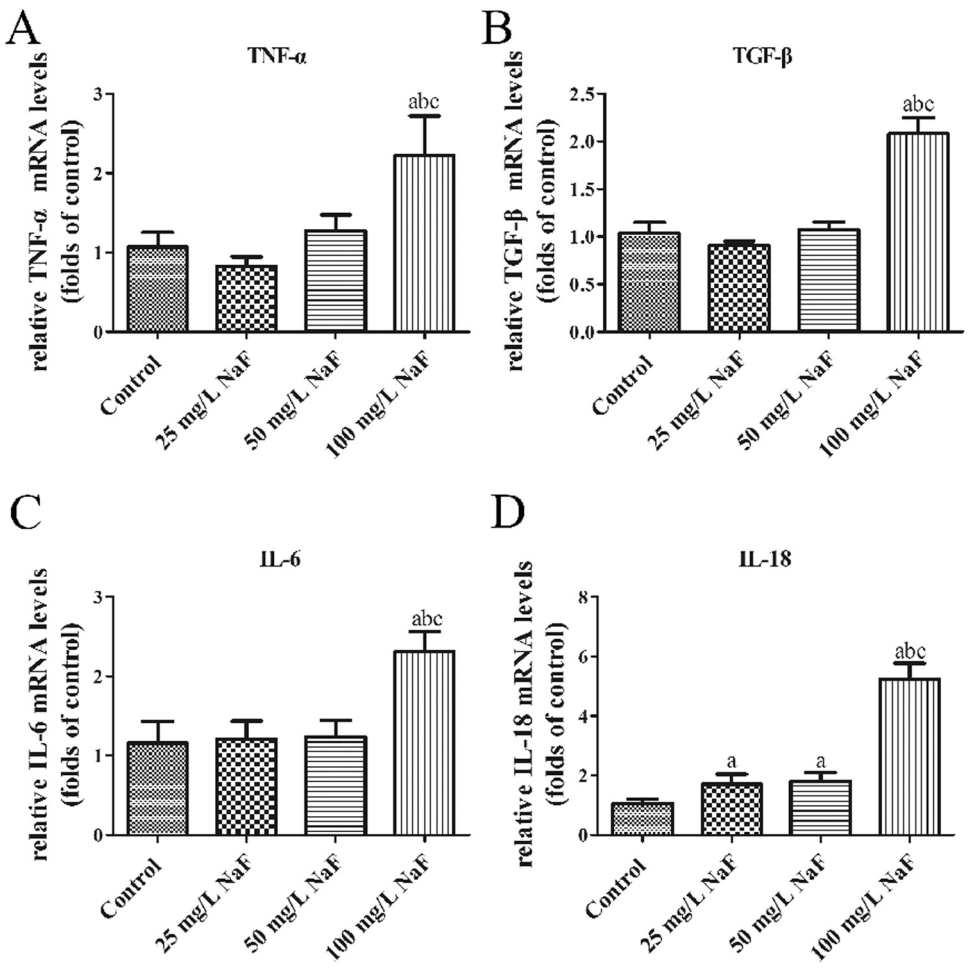

Fig. 8. Effects of fluoride on inflammatory cytokines in kidney. Mice were treated with 0, 25, 50 and 100 mg/L NaF-treated by drinking water for 5 months. The mRNA levels of tumor necrosis factor-α (TNF-α)(A), transforming growth factor-β(TGF-β)(B), interleukin-6 (IL-6)(C) and interleukin-6 (IL-18)(D) in kidney were determined by real-time PCR. Results were expressed as the mean ± SD (n = 6). [a] $P<0.05$ compared with the control mice. [b] $P<0.05$ compared with the 25 mg/L NaF-treated mice. [c] $P<0.05$ compared with the 50 mg/L NaF-treated mice.

upregulation of NLRP3, caspase-1 and IL-1β was observed in the kidneys after fluoride exposure. These findings highlight the involvement of NLRP3 inflammasome activation in fluoride-induced renal inflammation.

TNF-α is known to promote inflammation and tissue damage by inducing the expression of adhesion molecules and pro-inflammatory cytokines (Zelová and Hošek, 2013). TGF-β is a potent profibrotic cytokine that contributes to tissue fibrosis and extracellular matrix deposition (Peng et al., 2022). IL-6 is a pleiotropic cytokine involved in immune regulation, the acute-phase response and tissue repair (Yu et al., 2022). IL-18 is a pro-inflammatory cytokine belonging to the IL-1 family; it regulates both Th1 and Th2 responses (Vecchié et al., 2021). Owumi et al. found that adult male Wister rats exposed to 15 mg/L of NaF for 14 days had significantly elevated renal levels of NO, IL-1β and TNF-α (Owumi et al., 2019). In the study by Luo et al., ICR mice exposed to NaF at doses exceeding 12 mg/kg for 42 days showed alterations in the mRNA and protein expression levels of cyclooxygenase-2 (COX-2), TNF-α, IL-1β, IL-6 and interleukin-8 (IL-8) in the kidneys (Luo et al., 2017). In addition, increased secretions of proinflammatory factors including TNF-α, IL-6 and monocyte chemoattractant protein-1(MCP-1) also found in hyperuricemic nephropathy mice (Ren et al., 2021). Consistent with these studies, the current study found upregulation of inflammatory cytokines, including TNF-α, TGF-β and IL-6, in the kidneys following fluoride exposure. These results suggest that the activation of the NLRP3 inflammasome and excessive release of inflammatory factors could be involved in renal inflammation induced by fluoride.

Histone lysine crotonylation (Kcr) was first reported in 2011 in the top journal *Cell* by Zhao's team at the University of Chicago (Tan et al., 2011). It also modified proteins including important regulators of key processes such as cell cycle progression, chromatin remodeling, organization, and metabolic activity (Zhao et al., 2023). Growing evidence indicates that Kcr participates in renal injury and disease. Recent studies support the chromodomain Y-like transcription repressor and crotonyl-CoA hydratase CDYL could regulate its catalytic activity on histone Kcr, and thereby modulates disease progression in autosomal dominant polycystic kidney disease (ADPKD) (Dang et al., 2022). Ruiz-Andres et al. (2016) found that histone Kcr levels and Sirt3 mRNA expression were markedly increased in the kidneys of an acute kidney injury (AKI) animal model. Yang et al. (2021) found that T. gondii infection leads to an increase in HDAC2, which reduces histone crotonylation, particularly on H2BK12cr, and suppresses NF-κB activation, impacting macrophage proliferation. Histone acyltransferase P300/CBP can transfer the crotonyl group to the ε-amino group of a lysine residue, thereby regulating gene transcription, and Sirt and HDAC are also modifying enzymes of histone Kcr (Xu et al., 2017). In the study by Suzuki and Bartlett (2014), rats treated with fluoride (0, 50, and 100 ppm) in drinking water for six weeks demonstrated significantly increased Sirt1 expression and Sirt1 phosphorylation, resulting in the augmentation of Sirt1 deacetylase activity in ameloblast-derived cells. HDAC3 has been reported to regulate TIMAP (TGFβ-inhibited membrane-associated protein), thereby affecting macrophage M2 polarization markers, migration and phagocytosis (Yang et al., 2017).

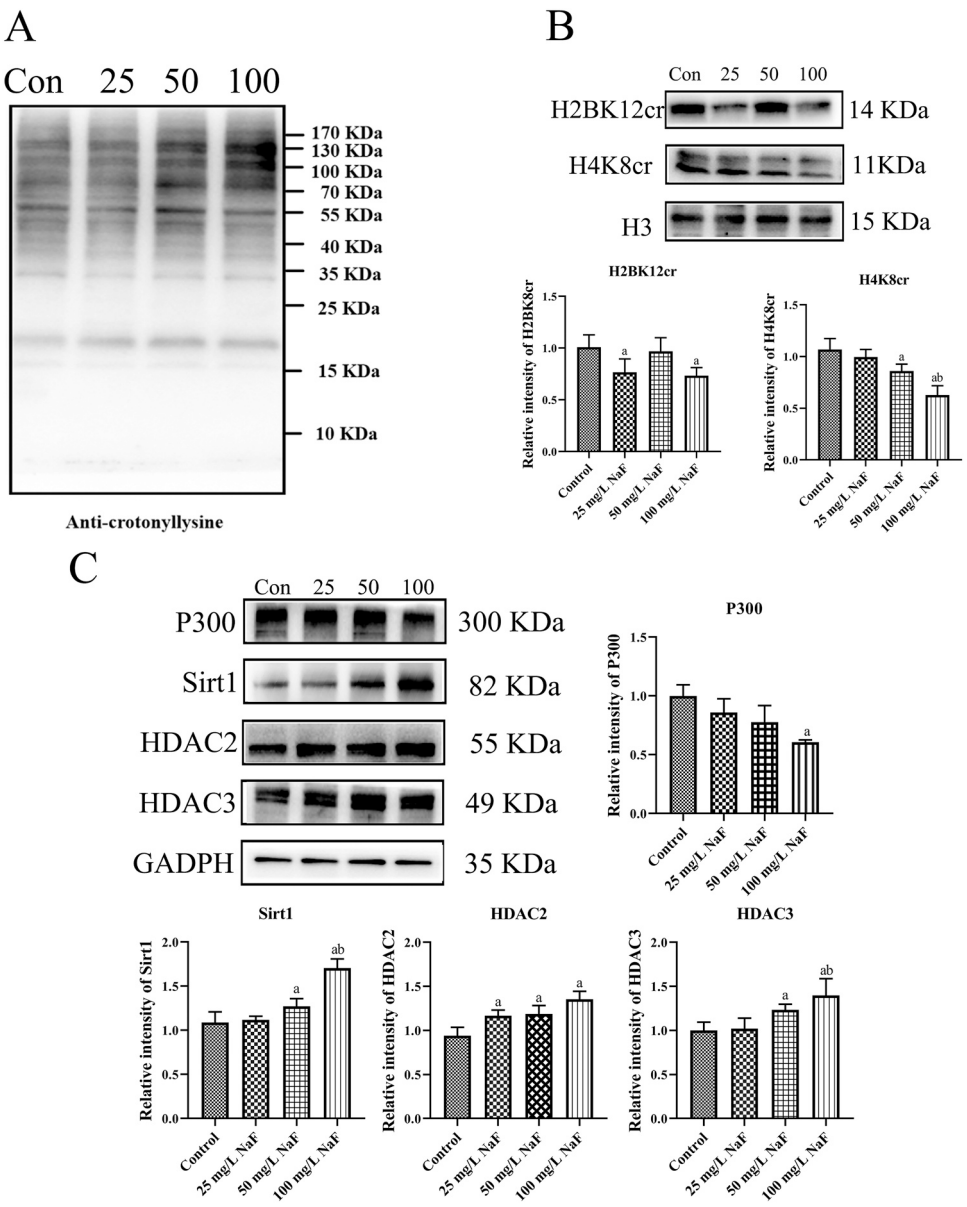

Fig. 9. Effects of fluoride on histone lysine crotonylation in kidney. Mice were treated with 0, 25, 50 and 100 mg/L NaF-treated by drinking water for 5 months. Expression of histone lysine crotonylation (A), H2BK12cr and H4K8cr (B) as well as ysine crotonylation-related enzymes P300, sirt1, HDAC2 and HDAC3 (C) in kidney were assessed by western blotting. H3 and GADPH was blotted as the loading control. The results were expressed as the mean ± SD (n = 4). [a] $P<0.05$ compared with the control mice.

Wang et al. (2024) used HDAC3$^{-/-}$ mice to confirm that HDAC3 can regulate the expression of proinflammatory cytokines (TNF-α, IL-1β, IL-6) and the number of CD45-marked bone marrow-derived leukocytes and F4/80-marked macrophages in the kidneys. Another study by Marumo et al. (2010) found that HDAC2 was upregulated in response to kidney injury and contributed to the induction of CSF-1, which, in turn, promoted macrophage infiltration and fibrotic responses. HDAC inhibition reduced CSF-1 levels, thereby decreasing macrophage infiltration and the associated inflammation and fibrosis in tubulointerstitial injury. In addition, HDAC1/HDAC2 can regulate CD4 lineage integrity and control CD4^{+} CTL differentiation (Preglej et al., 2020). In addition, Guan et al. found that the HDAC activity induce NLRP3 re-expression, which may be associated with HDAC-mediated chromatin condensation (Guan et al., 2024). These studies suggest that HDAC2 and HDAC3 are key regulators of kidney inflammation and immune responses. P300 is the first reported protein with histone crotonyltransferase activity (Xu et al., 2017). Liu et al. (2013) found that p300 affects Treg homeostasis or function, thereby promoting antitumour immunity. It has been reported that P300/CBP could regulate T cell lineages-related transcription factors T-BET, GATA3 and NFAT, as well as affect promoters of the pro-inflammatory cytokines such as IL-2, IL-4, and IFN-γ, play an important role in T cell activation (Picavet et al., 2024). The present experimental results showed that fluoride decreased the level of the histone crotonyltransferase P300 protein and upregulated the levels of the histone decrotonylation Sirt1 and the HDAC2 and HDAC3 proteins, thereby decreasing H2BK12cr and H4K8cr in the kidneys, and this process may be associated with fluoride-induced renal damage. However, the underlying regulation mechanism of histone lysine crotonylation about fluoride-induced renal toxocity should be validated in further studies.

5. Conclusions

A central finding in this study is that immune-inflammatory

imbalance by modulating Th1/Th2 differentiation and macrophage polarization, activating the NLRP3 inflammasome, and up-regulating the levels of inflammatory factors (TNF-a, TGF-β, IL-6 and IL-18) in the kidney are important components of fluoride-induced renaltoxicity, and this process may be associated with histone lysine crotonylation. These findings broaden our knowledge of renal immunotoxicity effects of fluoride and represent an attractive drug target for strategies to slow fluoride-induced kidney disease progression. Although we have tested the changes of histone lysine crotonylation modification including the related-enzymes and protein, but an in-depth understanding of the roles and mechanisms of Kcr in fluoride toxicity by interventions targeting these Kcr modification regulators will be the focus of our future study.

Statement

In all respects, the maintenance and treatment of animals were carried out in conformity with the guidelines for animal care, under a protocol authorized by the Ethics Committee of Shenyang Medical College(SYYXY2021031502).

Funding

This study was supported by grants from National Natural Science Foundation of China (NSFC) (No. 81803180), Liaoning Province Department of Science and Technology United Fund (NO. 2023-MSLH-292), Liaoning Provincial Economic and Social Development Research Project "Countermeasures and Paths for the Construction of Smart Precision Medicine in Liaoning Province Based on Big Data (No. 2024lslybkt-093), Liaoning Provincial Science and Technology Project Innovation Ability Improvement Joint Fund (NO. 2022-NLTS-14–06) , Shenyang Medical College Science and Technology Innovation Fund for postgraduate students (NO. Y20240527). Shenyang Science and technology plan project social governance science and technology special project (21-108-9-11).

CRediT authorship contribution statement

Zhenxiang Sun: Writing – review & editing, Data curation. **Shuang Yang:** Writing – review & editing, Investigation, Formal analysis. **Xiaoxu Duan:** Writing – review & editing, Validation, Supervision, Project administration, Funding acquisition. **Xinyue Wang:** Writing – review & editing, Supervision, Formal analysis. **Nan Yan:** Writing – review & editing, Validation, Supervision, Project administration, Funding acquisition. **Kangjie Xu:** Writing – review & editing, Investigation, Data curation. **Mingyue Ma:** Validation, Resources, Formal analysis. **Jingwen Zheng:** Writing – review & editing, Writing – original draft, Validation, Formal analysis, Data curation, Conceptualization. **Qian Wang:** Writing – review & editing, Formal analysis, Data curation. **Zhengdong Wang:** Visualization, Resources, Data curation.

Declaration of Competing Interest

The authors declare the following financial interests/personal relationships which may be considered as potential competing interests

Xiaoxu Duan reports financial support was provided by Liaoning Province Department of Science and Technology United Fund. Nan Yan reports financial support was provided by Liaoning Education Department Scientific Research Project. Nan Yan reports financial support was provided by The Central Government Guides Local Science and Technology Development Fund. Xiaoxu Duan reports financial support was provided by Shenyang Medical college student research project. If there are other authors, they declare that they have no known competing financial interests or personal relationships that could have appeared to influence the work reported in this paper.

Data availability

Data will be made available on request.

References

Aksoylar, H.I., Tijaro-Ovalle, N.M., Boussiotis, V.A., Patsoukis, N., 2020. Immunometabolism. T Cell Metab. Cancer Immunother. 2 (3), e200020.
Aulestia, F.J., Groeling, J., Bomfim, G.H.S., Costiniti, V., Manikandan, V., Chaloemtoem, A., Concepcion, A.R., Li, Y., Wagner, L.E., 2nd, Idaghdour, Y., Yule, D.I., Lacruz, R.S., 2020. Fluoride exposure alters Ca2+ signaling and mitochondrial function in enamel cells. Sci. Signal. 13, eaay0086.
Chaithra, B., Sarjan, H.N., Shivabasavaiah, 2020. Sodium fluoride and fluoride contaminated ground water induced altered reproductive performances in male rats. Biol. Trace Elem. Res. 195, 544–550.
Che, J., Yang, X., Jin, Z., Xu, C., 2023. Nrf2: A promising therapeutic target in bone-related diseases. Biomed. Pharmacother. 168, 115748.
Chen, J., Cao, J., Wang, J., Jia, R., Xue, W., Xie, L., 2015. Fluoride-induced apoptosis and expressions of caspase proteins in the kidney of carp (Cyprinus carpio). Environ. Toxicol. 30, 769–781.
Chen, L., Jia, P., Liu, Y., Wang, R., Yin, Z., Hu, D., Ning, H., Ge, Y., 2023. Fluoride exposure disrupts the cytoskeletal arrangement and ATP synthesis of HT-22 cell by activating the RhoA/ROCK signaling pathway. Ecotoxicol. Environ. Saf. 254, 114718.
Chen, X., Wei, W., Li, Y., Huang, J., Ci, X., 2019. Hesperetin relieves cisplatin-induced acute kidney injury by mitigating oxidative stress, inflammation and apoptosis. Chem. Biol. Interact. 308, 269–278.
Chow, F.Y., Nikolic-Paterson, D.J., Ma, F.Y., Ozols, E., Rollins, B.J., Tesch, G.H., 2007. Monocyte chemoattractant protein-1-induced tissue inflammation is critical for the development of renal injury but not type 2 diabetes in obese db/db mice. Diabetologia 50, 471–480.
Dahdouh, F., Belhamzaoui, K., Aouadi, L., Aldahmash, W., Harrath, A.H., Plavan, G., Smaali, M.E., Berrabah, H.D., 2023. Bee Venom Causes Oxidative Stress, Biochemical and Histopathological Changes in the Kidney of Mice. Physiol. Res. 72, 455–463.
Dang, L., Cao, X., Zhang, T., Sun, Y., Tian, S., Gong, T., Xiong, H., Cao, P., Li, Y., Yu, S., Yang, L., Zhang, L., Liu, T., Zhang, K., Liang, J., Chen, Y., 2022. Nuclear Condensation of CDYL Links Histone Crotonylation and Cystogenesis in Autosomal Dominant Polycystic Kidney Disease. J. Am. Soc. Nephrol. 33, 1708–1725.
Dharmaratne, R.W., 2019. Exploring the role of excess fluoride in chronic kidney disease: A review. Hum. Exp. Toxicol. 38, 269–279.
Du, C., Xiao, P., Gao, S., Chen, S., Chen, B., Huang, W., Zhao, C., 2022. High Fluoride Ingestion Impairs Bone Fracture Healing by Attenuating M2 Macrophage Differentiation. Front. Bioeng. Biotechnol. 10, 791433.
Duan, X., Xu, G., Li, J., Yan, N., Li, X., Liu, X., Li, B., 2022. Arsenic induces continuous inflammation and regulates Th1/Th2/Th17/Treg balance in liver and kidney in vivo. Mediat. Inflamm. 2022, 8414047.
Fang, Y., Xu, X., Ding, J., Yang, L., Doan, M.T., Karmaus, P.W.F., Snyder, N.W., Zhao, Y., Li, J.L., Li, X., 2021. Histone crotonylation promotes mesoendodermal commitment of human embryonic stem cells. Cell Stem Cell 28, 748–763.e7.
Farooq, M.A., Niazi, A.K., Akhtar, J., Saifullah, Farooq, M., Souri, Z., Karimi, N., Rengel, Z., 2019. Acquiring control: The evolution of ROS-Induced oxidative stress and redox signaling pathways in plant stress responses. Plant Physiol. Biochem. PPB 141, 353–369.
Fellows, R., Denizot, J., Stellato, C., Cuomo, A., Jain, P., Stoyanova, E., Balázsi, S., Hajnády, Z., Liebert, A., Kazakevych, J., Blackburn, H., Corrêa, R.O., Fachi, J.L., Sato, F.T., Ribeiro, W.R., Ferreira, C.M., Perée, H., Spagnuolo, M., Mattiuz, R., Matolcsi, C., Varga-Weisz, P., 2018b. Microbiota derived short chain fatty acids promote histone crotonylation in the colon through histone deacetylases. Nat. Commun. 9, 105.
Fellows, R., Denizot, J., Stellato, C., Cuomo, A., Jain, P., Stoyanova, E., Balázsi, S., Hajnády, Z., Liebert, A., Kazakevych, J., Blackburn, H., Corrêa, R.O., Fachi, J.L., Sato, F.T., Ribeiro, W.R., Ferreira, C.M., Perée, H., Spagnuolo, M., Mattiuz, R., Matolcsi, C., Varga-Weisz, P., 2018a. Microbiota derived short chain fatty acids promote histone crotonylation in the colon through histone deacetylases. Nat. Commun. 9, 105.
Foresto-Neto, O., Menezes-Silva, L., Leite, J.A., Andrade-Silva, M., Câmara, N.O.S., 2024. Immunology of Kidney Disease. Annu. Rev. Immunol.
Fu, J., Wu, H., 2023. Structural Mechanisms of NLRP3 Inflammasome Assembly and Activation. Annu. Rev. Immunol. 41, 301–316.
Funes, S.C., Rios, M., Escobar-Vera, J., Kalergis, A.M., 2018. Implications of macrophage polarization in autoimmunity. Immunology 154, 186–195.
Guan, X., Liu, R., Wang, B., Xiong, R., Cui, L., Liao, Y., Ruan, Y., Fang, L., Lu, X., Yu, X., Su, D., Ma, Y., Dang, T., Chen, Z., Yao, Y., Liu, C., Zhang, Y., 2024. Inhibition of HDAC2 sensitises antitumour therapy by promoting NLRP3/GSDMD-mediated pyroptosis in colorectal cancer. Clin. Transl. Med 14, e1692.
He, Y., Xie, Y., Zhou, T., Li, D., Cheng, X., Yang, P., Luo, C., Liu, Y., Guo, M., Wan, Q., Yan, P., Gao, C., Zhang, Y.Y., Sun, X.D., Xu, Y., Huang, W., 2024. Sodium Crotonate Alleviates Diabetic Kidney Disease Partially Via the Histone Crotonylation Pathway. Inflammation. Advance online publication.
Hu, Y., Yan, Z., He, Y., Li, Y., Li, M., Li, Y., Zhang, D., Zhao, Y., Ommati, M.M., Wang, J., Huo, M., Wang, J., 2023. Ameliorative effects of different doses of selenium against fluoride-triggered apoptosis and oxidative stress-mediated renal injury in rats

through the activation of Nrf2/HO-1/NQO1 signaling pathway. Food Chem. Toxicol. 174, 113647.
Joyce, E., Glasner, P., Ranganathan, S., Swiatecka-Urban, A., 2017. Tubulointerstitial nephritis: diagnosis, treatment, and monitoring. Pediatr. Nephrol. 32, 577–587.
Karadogan, B., Beyaz, S., Gelincik, A., Buyukozturk, S., Arda, N., 2022. Evaluation of oxidative stress biomarkers and antioxidant parameters in allergic asthma patients with different level of asthma control. J. Asthma 59, 663–672.
Kimura, T., Isaka, Y., Yoshimori, T., 2017. Autophagy and kidney inflammation. Autophagy 13, 997–1003.
Kolisnyk, I., Voloshin, O., Savchenko, I., Yanchevskyi, O., Rashidi, B., 2021. Enzymatic activity in microsomes, lipid peroxidation of mice hepatocytes under the sodium fluoride. Georgian Med. N. 310, 169–176.
Levey, A.S., Coresh, J., 2012. Chronic kidney disease. Lancet 379, 165–180.
Li, Y., Du, X., Zhao, Y., Wang, J., Wang, J., 2021. Fluoride Can Damage the Spleen of Mice by Perturbing Th1/Th2 Cell Balance. Biol. Trace Elem. Res. 199, 1493–1500.
Li, H., Fan, J., Zhao, Y., Yang, J., Xu, H., Manthari, R.K., Cheng, X., Wang, J., Wang, J., 2021. Calcium alleviates fluoride-induced kidney damage via FAS/FASL, TNFR/TNF, DR5/TRAIL pathways in rats. Ecotoxicol. Environ. Saf. 226, 112851.
Li, L., Xiang, T., Guo, J., Guo, F., Wu, Y., Feng, H., Liu, J., Tao, S., Fu, P., Ma, L., 2024. Inhibition of ACSS2-mediated histone crotonylation alleviates kidney fibrosis via IL-1β-dependent macrophage activation and tubular cell senescence. Nat. Commun. 15, 3200.
Li, X., Yang, J., Luo, H., Qiao, Y., Zhao, L., Cheng, C., Fu, W., Tan, Y., Wang, J., Liang, C., Zhang, J., 2024. Riboflavin Attenuates Fluoride-Induced Testicular Injury via Interleukin 17A-Mediated Classical Pyroptosis. J. Agric. Food Chem. 72, 6143–6154.
Liu, R., Cui, S.F., Gan, C.D., Yang, J.Y., 2023. Effect of exogenous Ca on the physiology and growth indicators of pakchoi under foliar and root fluorine stress. Environ. Geochem. Health 45, 5343–5356.
Liu, Y., Wang, L., Predina, J., Han, R., Beier, U.H., Wang, L.C., Kapoor, V., Bhatti, T.R., Akimova, T., Singhal, S., Brindle, P.K., Cole, P.A., Albelda, S.M., Hancock, W.W., 2013. Inhibition of p300 impairs Foxp3+T regulatory cell function and promotes antitumor immunity. Nat. Med. 19, 1173–1177.
Liu, J.L., Xia, T., Yu, Y.Y., Sun, X.Z., Zhu, Q., He, W., Zhang, M., Wang, A., 2005. The influence of environmental fluoride exposure on human health. Wei Sheng Yan Jiu 34, 287–288.
Luo, Q., Cui, H., Deng, H., Kuang, P., Liu, H., Lu, Y., Fang, J., Zuo, Z., Deng, J., Li, Y., Wang, X., Zhao, L., 2017. Sodium fluoride induces renal inflammatory responses by activating NF-κB signaling pathway and reducing anti-inflammatory cytokine expression in mice. Oncotarget 8, 80192–80207.
Ma, Y., Meng, X., Sowanou, A., Wang, J., Li, H., Li, A., Zhong, N., Yao, Y., Pei, J., 2023. Effect of Fluoride on the Expression of 8-Hydroxy-2′-Deoxyguanosine in the Blood, Kidney, Liver, and Brain of Rats. Biol. Trace Elem. Res. 201, 2904–2916.
Ma, H., Shi, Z., Dong, Y., Liang, R., Chen, J., Wang, J., Wang, J., 2016. Effect of Fluoride on Endocytosis and Surface Marker Expression Levels of Mouse B Cells In Vitro. Cell. Physiol. Biochem. 39, 596–603.
Ma, H., Wang, H., Zhang, H., Guo, H., Zhang, W., Hu, F., Yao, Y., Wang, D., Li, C., Wang, J., 2020. Effects of phenanthrene on oxidative stress and inflammation in lung and liver of female rats. Environ. Toxicol. 35, 37–46.
Ma, L., Zhang, R., Li, D., Qiao, T., Guo, X., 2021. Fluoride regulates chondrocyte proliferation and autophagy via PI3K/AKT/mTOR signaling pathway. Chem. Biol. Interact. 349, 109659.
Malin, A.J., Lesseur, C., Busgang, S.A., Curtin, P., Wright, R.O., Sanders, A.P., 2019. Fluoride exposure and kidney and liver function among adolescents in the United States: NHANES, 2013-2016. Environ. Int. 132, 105012.
Marumo, T., Hishikawa, K., Yoshikawa, M., Hirahashi, J., Kawachi, S., Fujita, T., 2010. Histone deacetylase modulates the proinflammatory and -fibrotic changes in tubulointerstitial injury. Am. J. Physiol. Ren. Physiol. 298, F133–F141.
Mohammadi, A., Sharifi, A., Pourpaknia, R., Mohammadian, S., Sahebkar, A., 2018. Manipulating macrophage polarization and function using classical HDAC inhibitors: Implications for autoimmunity and inflammation. Crit. Rev. Oncol. Hematol. 128, 1–18.
Myers, G.L., Miller, W.G., Coresh, J., Fleming, J., Greenberg, N., Greene, T., Hostetter, T., Levey, A.S., Panteghini, M., Welch, M., Eckfeldt, J.H., National Kidney Disease Education Program Laboratory Working Group, 2006. Recommendations for improving serum creatinine measurement: a report from the Laboratory Working Group of the National Kidney Disease Education Program. Clin. Chem. 52, 5–18.
Nabavi, S.M., Nabavi, S.F., Habtemariam, S., Moghaddam, A.H., Latifi, A.M., 2012. Ameliorative effects of quercetin on sodium fluoride-induced oxidative stress in rat`s kidney. Ren. Fail. 34, 901–906.
Ntorla, A., Burgoyne, J.R., 2021. The regulation and function of histone crotonylation. Front. Cell Dev. Biol. 9, 624914.
Owumi, S.E., Aliyu-Banjo, N.O., Danso, O.F., 2019. Fluoride and diethylnitrosamine coexposure enhances oxido-inflammatory responses and caspase-3 activation in liver and kidney of adult rats. J. Biochem. Mol. Toxicol. 33, e22327.
Peng, D., Fu, M., Wang, M., Wei, Y., Wei, X., 2022. Targeting TGF-β signal transduction for fibrosis and cancer therapy. Mol. Cancer 21, 104.
Peres, R.A.S., Silva-Aguiar, R.P., Teixeira, D.E., Peruchetti, D.B., Alves, S.A.S., Leal, A.B. C., Castro, G.F., Ribeiro, N.B.S., Guimarães, F.V., Pinheiro, A.A.S., Silva, P.M.R.E., Martins, M.A., Caruso-Neves, C., 2023. Gold nanoparticles reduce tubule-interstitial injury and proteinuria in a murine model of subclinical acute kidney injury. Biochim. Biophys. Acta Gen. Subj. 1867, 130314.
Picavet, L.W., Samat, A.A.K., Calis, J., Nijhuis, L., Scholman, R., Mokry, M., Tough, D.F., Prinjha, R.K., Vastert, S.J., van Loosdregt, J., 2024. CBP/P300 Inhibition Impairs $CD4^+$ T Cell Activation: Implications for Autoimmune Disorders. Biomedicines 126, 1344.
Piesiak-Pańczyszyn, D., Zakrzewski, W., Piszko, A., Piszko, P.J., Dobrzyński, M., 2023. Review on fluoride varnishes currently recommended in dental prophylaxis. Polim. Med. 53, 141–151.
Preglej, T., Hamminger, P., Luu, M., Bulat, T., Andersen, L., Göschl, L., Stolz, V., Rica, R., Sandner, L., Waltenberger, D., Tschismarov, R., Faux, T., Boenke, T., Laiho, A., Elo, L.L., Sakaguchi, S., Steiner, G., Decker, T., Bohle, B., Visekruna, A., Ellmeier, W., 2020. Histone deacetylases 1 and 2 restrain CD4+ cytotoxic T lymphocyte differentiation. JCI Insight 5, e133393.
Qu, L., Jiao, B., 2023. The Interplay between Immune and Metabolic Pathways in Kidney Disease. Cells 12, 1584.
Qujeq, D., Laghaie, B., Gholipour, A., Solimani, N., Hassenzadeh, S., 2002. Effects of sodium fluoride on total serum protein levels and transaminase activity in rats. Biomed. Pharmacother. 56, 169–172.
Ramasubramanian, R., Kalhan, R., Jacobs, D.R., Jr, Washko, G.R., Hou, L., Gross, M.D., Guan, W., Thyagarajan, B., 2021. Gene expression of oxidative stress markers and lung function: A CARDIA lung study. Mol. Genet. Genom. Med. 9, e1832.
Ren, Q., Tao, S., Guo, F., Wang, B., Yang, L., Ma, L., Fu, P., 2021. Natural flavonol fisetin attenuated hyperuricemic nephropathy via inhibiting IL-6/JAK2/STAT3 and TGF-β/SMAD3 signaling. Phytomedicine 87, 153552.
Ruiz-Andres, O., Sanchez-Niño, M.D., Cannata-Ortiz, P., Ruiz-Ortega, M., Egido, J., Ortiz, A., Sanz, A.B., 2016. Histone lysine crotonylation during acute kidney injury in mice. Dis. Model. Mech. 9, 633–645.
Sabari, B.R., Tang, Z., Huang, H., Yong-Gonzalez, V., Molina, H., Kong, H.E., Dai, L., Shimada, M., Cross, J.R., Zhao, Y., Roeder, R.G., Allis, C.D., 2015. Intracellular crotonyl-CoA stimulates transcription through p300-catalyzed histone crotonylation. Mol. Cell 58, 203–215.
Santoyo-Sanchez, M.P., Silva-Lucero, M.C., Arreola-Mendoza, L., Barbier, O.C., 2013. Effects of acute sodium fluoride exposure on kidney function, water homeostasis, and renal handling of calcium and inorganic phosphate. Biol. Trace Elem. Res. 152, 367–372.
Shang, Q., Yu, X., Sun, Q., Li, H., Sun, C., Liu, L., 2024. Polysaccharides regulate Th1/Th2 balance: A new strategy for tumor immunotherapy. Biomed. Pharmacother. 170, 115976.
Shao, D., Zhang, J., Tang, L., Yu, Q., Hu, X., Ruan, Q., Ouyang, W., Zhang, Z., 2020. Effects and molecular mechanism of L-type calcium channel on fluoride-induced kidney injury. Biol. Trace Elem. Res. 197, 213–223.
Shapouri-Moghaddam, A., Mohammadian, S., Vazini, H., Taghadosi, M., Esmaeili, S.A., Mardani, F., Seifi, B., Mohammadi, A., Afshari, J.T., Sahebkar, A., 2018. Macrophage plasticity, polarization, and function in health and disease. J. Cell. Physiol. 233, 6425–6440.
Singh, V., Ubaid, S., 2020. Role of silent information regulator 1 (SIRT1) in regulating oxidative stress and inflammation. Inflammation 43, 1589–1598.
Solanki, Y.S., Agarwal, M., Gupta, A.B., Gupta, S., Shukla, P., 2022. Fluoride occurrences, health problems, detection, and remediation methods for drinking water: A comprehensive review. Sci. Total Environ. 807, 150601.
Suárez-Fueyo, A., Bradley, S.J., Klatzmann, D., Tsokos, G.C., 2017. T cells and autoimmune kidney disease. Nat. Rev. Nephrol. 13, 329–343.
Sun, L., Su, Y., Jiao, A., Wang, X., Zhang, B., 2023. T cells in health and disease. Signal Transduct. Target. Ther. 8, 235.
Suzuki, M., Bartlett, J.D., 2014. Sirtuin1 and autophagy protect cells from fluoride-induced cell stress. Biochim. Biophys. Acta 1842, 245–255.
Tan, M., Luo, H., Lee, S., Jin, F., Yang, J.S., Montellier, E., Buchou, T., Cheng, Z., Rousseaux, S., Rajagopal, N., Lu, Z., Ye, Z., Zhu, Q., Wysocka, J., Ye, Y., Khochbin, S., Ren, B., Zhao, Y., 2011. Identification of 67 histone marks and histone lysine crotonylation as a new type of histone modification. Cell 146, 1016–1028.
Vecchié, A., Bonaventura, A., Toldo, S., Dagna, L., Dinarello, C.A., Abbate, A., 2021. IL-18 and infections: Is there a role for targeted therapies? J. Cell. Physiol. 236, 1638–1657.
Wang, D., Cao, L., Zhou, X., Wang, G., Ma, Y., Hao, X., Fan, H., 2022a. Mitigation of honokiol on fluoride-induced mitochondrial oxidative stress, mitochondrial dysfunction, and cognitive deficits through activating AMPK/PGC-1α/Sirt3. J. Hazard. Mater. 437, 129381.
Wang, D., Cao, L., Zhou, X., Wang, G., Ma, Y., Hao, X., Fan, H., 2022b. Mitigation of honokiol on fluoride-induced mitochondrial oxidative stress, mitochondrial dysfunction, and cognitive deficits through activating AMPK/PGC-1α/Sirt3. J. Hazard. Mater. 437, 129381.
Wang, Y., Jiao, B., Hu, Z., Wang, Y., 2024. Critical role of histone deacetylase 3 in the regulation of kidney inflammation and fibrosis. Kidney Int 105, 775–790.
Wang, C., Pan, Y., Zhang, Q.Y., Wang, F.M., Kong, L.D., 2012. Quercetin and allopurinol ameliorate kidney injury in STZ-treated rats with regulation of renal NLRP3 inflammasome activation and lipid accumulation. PLoS One 7, e38285.
Wang, X., Tewari, N., Sato, F., Tanimoto, K., Thangavelu, L., Makishima, M., Bhawal, U. K., 2022d. Biphasic functions of sodium fluoride (NaF) in soft and in hard periodontal tissues. Int. J. Mol. Sci. 23, 962.
Wang, G., Wang, T., Zhang, X., Chen, J., Feng, C., Yun, S., Cheng, Y., Cheng, F., Cao, J., 2022c. Sex-specific effects of fluoride and lead exposures on histology, antioxidant physiology, and immune system in the liver of zebrafish (Danio rerio). Ecotoxicology 31, 396–414.
Wang, H.W., Zhu, S.Q., Liu, J., Miao, C.Y., Zhang, Y., Zhou, B.H., 2020. Fluoride-induced renal dysfunction via respiratory chain complex abnormal expression and fusion elevation in mice. Chemosphere 238, 124607.
Weiss-Sadan, T., Ge, M., Hayashi, M., Gohar, M., Yao, C.H., de Groot, A., Harry, S., Carlin, A., Fischer, H., Shi, L., Wei, T.Y., Adelmann, C.H., Wolf, K., Vornbäumen, T., Dürr, B.R., Takahashi, M., Richter, M., Zhang, J., Yang, T.Y., Vijay, V., Bar-Peled, L., 2023. NRF2 activation induces NADH-reductive stress, providing a metabolic vulnerability in lung cancer. Cell Metab. 35, 487–503.e7.

Wu, L., Fan, C., Zhang, Z., Zhang, X., Lou, Q., Guo, N., Huang, W., Zhang, M., Yin, F., Guan, Z., Yang, Y., Gao, Y., 2021. Association between fluoride exposure and kidney function in adults: A cross-sectional study based on endemic fluorosis area in China. Ecotoxicol. Environ. Saf. 225, 112735.
Xu, J., Núñez, G., 2023. The NLRP3 inflammasome: activation and regulation. Trends Biochem. Sci. 48, 331–344.
Xu, W., Wan, J., Zhan, J., Li, X., He, H., Shi, Z., Zhang, H., 2017. Global profiling of crotonylation on non-histone proteins. Cell Res 27, 946–949.
Yan, X., Chen, X., Tian, X., Qiu, Y., Wang, J., Yu, G., Dong, N., Feng, J., Xie, J., Nalesnik, M., Niu, R., Xiao, B., Song, G., Quinones, S., Ren, X., 2021. Co-exposure to inorganic arsenic and fluoride prominently disrupts gut microbiota equilibrium and induces adverse cardiovascular effects in offspring rats. Sci. Total Environ. 767, 144924.
Yang, J., He, Z., Chen, C., Li, S., Qian, J., Zhao, J., Fang, R., 2021. Toxoplasma gondii infection inhibits histone crotonylation to regulate immune response of porcine alveolar macrophages. Front. Immunol. 12, 696061.
Yang, J., Yin, S., Bi, F., Liu, L., Qin, T., Wang, H., Cao, W., 2017. TIMAP repression by TGFβ and HDAC3-associated Smad signaling regulates macrophage M2 phenotypic phagocytosis. J. Mol. Med. 95, 273–285.
Yu, H., Bu, C., Liu, Y., Gong, T., Liu, X., Liu, S., Peng, X., Zhang, W., Peng, Y., Yang, J., He, L., Zhang, Y., Yi, X., Yang, X., Sun, L., Shang, Y., Cheng, Z., Liang, J., 2020. Global crotonylome reveals CDYL-regulated RPA1 crotonylation in homologous recombination-mediated DNA repair. Sci. Adv. 6, eaay4697.
Yu, Y., Niu, R., Zhao, F., Zhao, Y., Wang, J., Wang, J., Cao, Q., Fu, R., Nateghahmadi, M. H., Sun, Z., 2022. Moderate exercise relieves fluoride-induced liver and kidney inflammatory responses through the IKKβ/NFκB pathway. Environ. Sci. Pollut. Res. 29, 78429–78443.
Zelová, H., Hošek, J., 2013. TNF-α signalling and inflammation: interactions between old acquaintances. Inflamm. Res. 62, 641–651.
Zhang, Y., Dong, F., Wang, Z., Xu, B., Zhang, T., Wang, Q., Lin, Q., 2023. Fluoride exposure provokes mitochondria-mediated apoptosis and increases mitophagy in osteocytes via increasing ROS production. Biol. Trace Elem. Res. 201, 3994–4007.
Zhang, Q., Li, T., Shi, R., Qi, R., Hao, X., Ma, B., 2024. Fluoride promotes the secretion of inflammatory factors in microglia through NLRP3/Caspase-1/GSDMD pathway. Environ. Sci. Pollut. Res. Int 31, 19844–19855.
Zhang, R., Liu, X., Ma, Y., Cheng, L., Ren, Y., Li, R., 2023. Identification of Cell-Cell Communications by Single-Cell RNA Sequencing in End Stage Renal Disease Provides New Insights into Immune Cell Heterogeneity. J. Inflamm. Res. 16, 4977–5000.
Zhang, Y., Yang, W., Li, W., Zhao, Y., 2021. NLRP3 inflammasome: Checkpoint connecting innate and adaptive immunity in autoimmune diseases. Front. Immunol. 12, 732933.
Zhao, H., Han, Y., Zhou, P., Guan, H., Gao, S., 2023. Protein lysine crotonylation in cellular processions and disease associations. Genes Dis. 11, 101060.
Zhao, L., Yu, Y., Deng, C., 2014. Protein and mRNA expression of Shh, Smo and Gli1 and inhibition by cyclopamine in hepatocytes of rats with chronic fluorosis. Toxicol. Lett. 225, 318–324.
Zuk, A., Bonventre, J.V., 2016. Acute kidney injury. Annu. Rev. Med. 67, 293–307.